Cambridge Centre for Computational Chemical Engineering

University of Cambridge

Department of Chemical Engineering

Preprint ISSN 1473 – 4273

Incorporating experimental uncertainties into multivariate granulation modelling

Andreas Braumann [1] Markus Kraft [1]

released: 29 January 2009

[1] Department of Chemical Engineering
University of Cambridge
New Museums Site
Pembroke Street
Cambridge, CB2 3RA
UK
E-mail: mk306@cam.ac.uk

Preprint No. 66

c4e

Key words and phrases: agglomeration, error propagation, granulation, parameter identification, particulate processes, population balance

Edited by
Cambridge Centre for Computational Chemical Engineering
Department of Chemical Engineering
University of Cambridge
Cambridge CB2 3RA
United Kingdom.

Fax: + 44 (0)1223 334796
E-Mail: c4e@cheng.cam.ac.uk
World Wide Web: http://www.cheng.cam.ac.uk/c4e/

Abstract

A methodology that carries experimental uncertainties into model predictions is studied and applied to a multidimensional population balance model for granulation processes. This complex model contains 27 parameters. A portion of them such as material constants can be measured or estimated, whereas some of the model parameters need to be established through granulation experiments and subsequent fitting to the model. As uncertainties are associated with every measurement, these are used in the presented methodology for the computation of uncertainties in the model predictions. This allows one to assess the quality of a model and to identify outliers in the experimental observations. As the evaluation of the complex model framework is computationally expensive, the granulation process is approximated with response surfaces in the studied example, allowing the quick computation of the model response in the optimisation procedure. Using eight sets of experimental observations, model-specific rate constants for particle coalescence, compaction, breakage, and reaction are calculated. Additionally, uncertainties of these parameters are estimated, allowing for the calculation of the model prediction and its uncertainty. Whereas the *a priori* uncertainties are relatively large, the uncertainties are significantly reduced by the method proposed. In addition to this, a possible mismatch between the model and the experimental observations is identified, giving hints for further investigations.

Contents

1 Introduction

Mathematical models are widely used in chemical engineering to describe the state of systems and the changes that occur due to various processes acting in the systems. The set of equations in such a model framework very often contains system-specific parameters that are not known *a priori*. The estimation of these parameters is known as the inverse problem and is encountered for all kinds of models. Amongst the more complex model equations are population balance equations—integro-differential equations describing the evolution of a population of individual entities such as particles, bubbles or even biological cells [25]. Population balances are applied to many processes, examples being extraction [36] and granulation [5, 7]. Granulation is a widely used process which transforms particles into bigger entities and thereby improves their properties [19]. However, in the modelling of granulation processes the inverse problem is often unavoidable. Therefore experiments have to be carried out in order to identify these unknown model parameters, e. g. coalescence rate constants. Such parameter estimation is normally done through fitting to the model [2, 27]. Once these model parameters are determined, the model can be employed for the study of the system under consideration. For instance, one may want to investigate the sensitivity of the process with respect to certain process conditions and/or model parameters, as is common practice for a wide range of models in chemical engineering [32]. In order to study the sensitivity of coagulation processes, which also occur in granulation, Monte Carlo techniques offer an attractive way forward [17, 34, 35].

When experimental observations are made, there are always uncertainties associated with them. This means, the value stated for an observation is the most likely one to occur, but at the same time it can also take other values (within the level of confidence). If this experimental observation is used for the estimation of a model parameter when solving the inverse problem, the experimental uncertainty should result in some kind of uncertainty in the model parameter. In order to study such process behaviour with uncertain model parameters, Monte Carlo simulations present a feasible way. This technique is for instance used by Phenix *et al.* [23], modelling the oxidation kinetics in supercritical water. As such, ranges for several model parameters are defined, and combinations of parameter values are drawn according to the distributions of the parameters. For each of these several thousand sets, the model equations (ODEs) are solved. From the results (= model predictions) statistics can be derived providing mean values of the model predictions and the associated uncertainties. In order to study the sensitivities of the model predictions with respect to the model parameter uncertainties, a polynomial chaos expansion may be added to the framework [26]. Therefore each uncertain parameter is expressed by random variables from a known probability density, so that the model solution can be decomposed, revealing the influence of the uncertainties in the model parameters on the uncertainty in the model solution. However, the drawback of the Monte Carlo simulations still persists, namely the computational costs arising from the large number of simulations that have to be performed. In order to counteract the need for a large number of model evaluations, tabulation techniques may be employed [21]. Model solutions for selected parameter combinations are stored in an appropriate way, so that the model prediction for the parameter combination in question can be obtained from interpolation between the tabulated solutions.

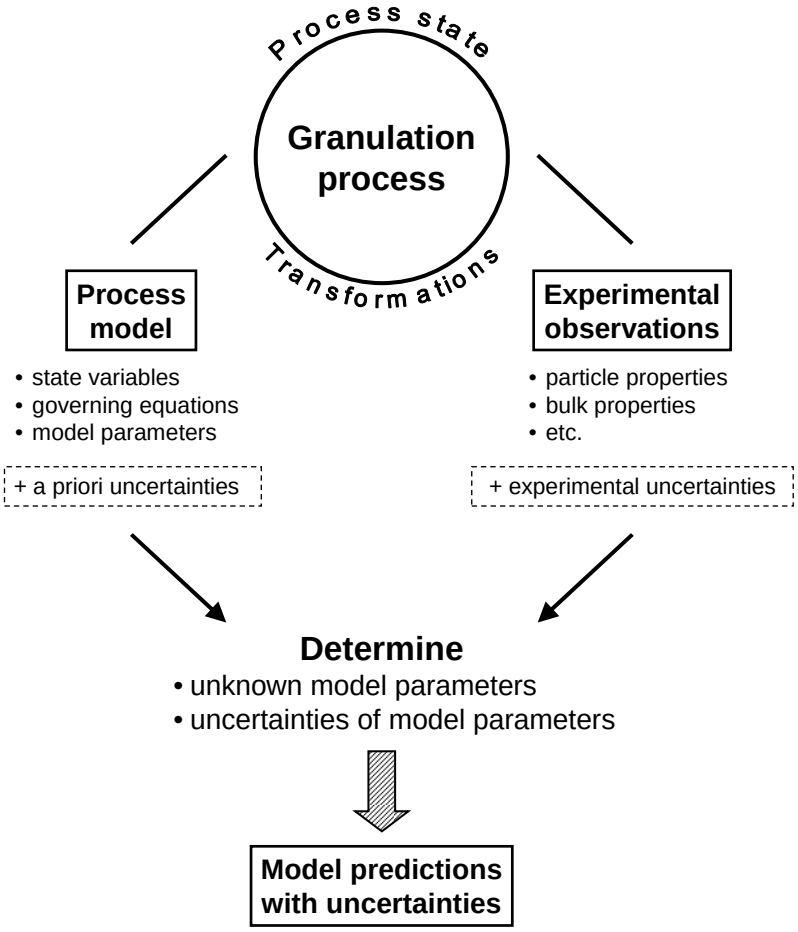

Figure 1: *Outline of the problem and the employed methodology*

The ultimate aim of any model development is the arrival of a robust, reliable and precise framework applicable to a variety of problems and conditions. This means the parameters for such framework should be estimated as accurately as necessary, so that the uncertainty in any model prediction is small. In a first step one may predefine the uncertainties of the model parameters in order to study the uncertainty in the model predictions [23, 26]. These *a priori* uncertainties of the model parameters mark the range in which the hitherto unknown values for the model parameters of question will fall. These ranges have to be estimated by the user.

The **purpose of this paper** is to show how experimental uncertainties can be used for the refinement and reduction of the uncertainty intervals of the model parameters, and the model prediction for the modelling of multidimensional granulation problems. In the employed methodology the experimental observations are exploited for the derivation of the values of the model parameters and their uncertainties, allowing predictions with the refined model (**Figure 1**). A simple polynomial chaos expansion in the model parameters is introduced, so that the unknown values of the model parameters and their uncertainties can be estimated using a standard least-square routine. In this, the model response is provided by response surfaces, so that the model evaluation becomes computationally cheap. As such, we follow the approach proposed by Sheen *et al.* [29]. The application of the

methodology is demonstrated for an example from wet granulation for which the inverse problem is solved. The unknown model parameters are rate constants for various transformations being incorporated in the model, namely for coalescence, compaction, breakage, and chemical reaction. As such, the influence of the used experimental observations on the parameter estimation is studied by different selections of experimental sets. These sets differ not only in time, but also in the process conditions, i. e., variations in the impeller speed. As a result of this, different sets of model parameters and their uncertainties can be extracted, so that for each of them, model predictions can be derived. This methodology allows for comparison between the different scenarios. In addition to this, it has the potential that the quality of a model can be assessed and outliers in the experiments can be identified, thereby suggesting future steps, such as model refinement, to be taken in addressing the problem.

2 Theory

2.1 Uncertainty analysis

In order to estimate the unknown value of a model parameter using an optimisation procedure, an experimental observation is needed. This experimental observation η^{exp} is characterised by two parameters, the measured value η_0^{exp} and its uncertainty σ^{exp}, so that the experimental observation can be written as,

$$\eta^{\text{exp}} = \eta_0^{\text{exp}} \pm \sigma^{\text{exp}} \quad . \tag{1}$$

Secondly, a model response η will be required for the model parameter estimation. This model response is the process model evaluated for a given set of model parameters, $\boldsymbol{x}$,

$$\boldsymbol{x} = (x_1, \ldots, x_K) \quad , \tag{2}$$

so that

$$\eta = \eta(\boldsymbol{x}) \quad . \tag{3}$$

Due to the experimental uncertainty σ^{exp} there will be more than one set $\boldsymbol{x}^*$ that will lead to a match between the experimental observation η^{exp} and the model response η. This means the uncertainty in the experimental observation σ^{exp} causes the uncertainty in the choice of the model parameters. Hence some uncertainty must be allowed in the model itself and this is introduced through the model parameters. Therefore a model parameter x is represented as

$$x = x_0 + c\,\xi \quad , \tag{4}$$

with x_0 as the base value, a uncertainty factor c and the random variable ξ. Expressing the model parameter x by eq. (4) is the simplest form of a polynomial chaos expansion [38]. As result of this representation, x becomes a random variable itself. The random variable ξ shall be standard normally distributed. The model response η can now be rewritten as,

$$\eta(\boldsymbol{x}) = \eta(\boldsymbol{x_0}, \boldsymbol{c}, \boldsymbol{\xi}) \quad . \tag{5}$$

Due to the dependency on $\boldsymbol{\xi}$ the model response becomes also a random variable. However, the model prediction should be represented by just one value and its associated uncertainty. Taking the expectation of the model response and the variance respectively leads to the model prediction, μ,

$$\mu(\boldsymbol{x_0}, \boldsymbol{c}) = E\left[\eta(\boldsymbol{x_0}, \boldsymbol{c}, \boldsymbol{\xi})\right] \quad , \tag{6}$$

and the model uncertainty σ,

$$\sigma(\boldsymbol{x_0}, \boldsymbol{c}) = \sqrt{\mathrm{Var}\left(\eta(\boldsymbol{x_0}, \boldsymbol{c}, \boldsymbol{\xi})\right)} \quad . \tag{7}$$

Often processes are described by differential equations, so it is the case for granulation. The temporal evolution of the particles may be modelled using population balance equations, which themselves are integro-differential equations. The problem that arises is that the evaluation of these equations is often computationally expensive. In order to overcome this difficulty, an approximation of the process behaviour by response surfaces is proposed. This approach can be followed because the ranges for the unknown parameters $\boldsymbol{x}$ are roughly known.

2.2 Model approximation by response surfaces

Response surfaces are simple models that approximate the behaviour of a system within predefined boundaries [18]. A system is defined by a set of points that are either observations from an experiment or responses from a model. As such, these points are distinguished from each other by different process conditions and/or choice of model parameters. These so called design variables are normally expressed in a normalised way, so that none of them carries any physical dimension, and hence they are called coded variables. In the present case the model parameters $\boldsymbol{x}$ are the design variables, and for further consideration it is assumed that they are coded variables.

The simplest response surface is linear in nature. This means the model response $\eta(\boldsymbol{x})$ can be approximated by,

$$\eta(\boldsymbol{x}) = \beta_0 + \sum_{k=1}^{K} \beta_k \, x_k \quad , \tag{8}$$

with β_0 and β_k $(k = 1, \ldots, K)$ being the parameters of the response surface. The response surface parameters β_0 and β_k are obtained by fitting the surface to the set of points of the system of interest. Before this can be done, the variables that distinguish the observations of the system need to be transformed into coded variables, which are dimensionless. Thus, the parameters β_0 and β_k $(k = 1, \ldots, K)$ have the same dimension as the response $\eta(\boldsymbol{x})$. After introduction of eq. (4) into eq. (8) the model response takes following form

$$\eta(\boldsymbol{x_0}, \boldsymbol{c}, \boldsymbol{\xi}) = \beta_0 + \sum_{k=1}^{K} \beta_k \cdot (x_{0,k} + c_k \, \xi_k) \quad . \tag{9}$$

The mean value μ and the uncertainty σ are obtained after taking the expectation and the variance respectively,

$$\mu(\boldsymbol{x_0}) = E\left[\eta\left(\boldsymbol{x_0}, \boldsymbol{c}, \boldsymbol{\xi}\right)\right] = \beta_0 + \sum_{k=1}^{K} \beta_k \, x_{0,k} \quad , \tag{10}$$

$$\sigma(\boldsymbol{c}) = \sqrt{\mathrm{Var}\left(\eta(\boldsymbol{x_0}, \boldsymbol{c}, \boldsymbol{\xi})\right)} = \sqrt{\sum_{k=1}^{K} \beta_k^2 \, c_k^2} \quad . \tag{11}$$

This means the most likely model solutions fall within the interval

$$\eta(\boldsymbol{x}) = \mu(\boldsymbol{x_0}) \pm \sigma(\boldsymbol{c}) \quad , \tag{12}$$

$$= \beta_0 + \sum_{k=1}^{K} \beta_k \, x_{0,k} \pm \sqrt{\sum_{k=1}^{K} \beta_k^2 \, c_k^2} \quad . \tag{13}$$

A short explanation of how to derive the mean and the uncertainty is given in appendix A. The task that remains is to find the optimal values of $\boldsymbol{x_0}$ and $\boldsymbol{c}$ using an appropriate objective function.

2.3 Objective function

Before formulating any objective function, we have a quick look how the problem presents itself to us. Any system—in the current study a granulation process—can be described by experimental observations. In the case of granulation this can be information about the particles such as the amount of oversize or undersize. However, the system can also be described by a model. In this, the process is characterised by state variables and governing equations. The overall aim of the modelling work is to come up with a robust and precise model that allows predictions for various kinds of cases. Hence, the model parameters and their uncertainties shall be estimated using a set of experimental observations (cf. Figure 1). In the current situation it is assumed that some prior knowledge about the ranges of the parameters $\boldsymbol{x}$ and their uncertainties $\boldsymbol{c}$ exists.

This means the aim of the optimisation is twofold. On the one hand optimal values for the model parameters $\boldsymbol{x_0}$ need to be found, i. e., the model predictions should be as close as possible to the experimental observation. On the other hand we wish to find the uncertainty of the parameters, i. e., reduce the *a priori* uncertainty, exploiting the uncertainty of the experimental observations. This is achieved by minimising the difference between the uncertainties of the experiment and model prediction. Hence the objective function Φ takes following form,

$$\Phi(\boldsymbol{x_0}, \boldsymbol{c}) = \sum_{i=1}^{N} \left(\left[\eta_i^{\mathrm{exp}} - \mu_i(\boldsymbol{x_0})\right]^2 + \left[\sigma_i^{\mathrm{exp}} - \sigma_i(\boldsymbol{c})\right]^2 \right) \tag{14}$$

with $i = 1, \ldots, N$ being the index and N the number of the experimental observations. Other objective functions are conceivable, but beyond the scope of the current study. The

optimum $(\boldsymbol{x}_0^*, \boldsymbol{c}^*)$ originates from,

$$(\boldsymbol{x}_0^*, \boldsymbol{c}^*) = \underset{\boldsymbol{x_0}, \boldsymbol{c}}{\operatorname{argmin}} \{\Phi(\boldsymbol{x_0}, \boldsymbol{c})\} \quad . \tag{15}$$

The optimisation procedure is subject to some constraints. The variables $\boldsymbol{x_0}$ can only take values within the prior defined range,

$$x_{0,k,\text{low}} \leq x_{0,k} \leq x_{0,k,\text{up}} \qquad (k = 1, \ldots, K) \quad . \tag{16}$$

The uncertainty parameters $\boldsymbol{c}$ cannot become negative. In addition to this, they are bound by the *a priori* estimates $\boldsymbol{c^{(0)}}$,

$$0 \leq \boldsymbol{c} \leq \boldsymbol{c^{(0)}} \quad . \tag{17}$$

3 Application to multidimensional granulation modelling

The methodology outlined above is applied to an example from granulation modelling.

3.1 The granulation process and its modelling

Broadly speaking, granulation is the clustering of small particles into bigger entities, commonly called granules. These bigger particles have enhanced properties in comparison to a simple mixture of all the small particles. Beneficial properties of granules are for instance a gain in safety, transport properties and application properties. In terms of safety, the formation of granules is meant to reduce the dustiness of the particle handling process, and therefore also reduces the risk of dust explosions, as well as the exposure of human beings and the environment to dust. Granulation "freezes" the composition of particles within the granules, so that problems like segregation during transport of particle mixtures can be eradicated. With respect to the application properties dissolution behaviour and controlled release are on the forefront, being crucial properties in many industries ranging from pharmaceuticals to food and detergent products.

Over the years various types of equipment have been being used for granulation processes. The type of equipment used for the process basically determines which shear rates are acting on the particles [31]. Drum granulation is seen as the most gentle treatment of the particles and is for instance used for the granulation of fertilizers and ores [1, 37]. The particles experience higher shear rates when the process is carried out in a fluidised bed. This kind of equipment is used for a wide range of products such as detergents [4] and pharmaceuticals [3]. For the production of dense granules, high-shear granulation is the preferred method [20]. Depending on the application, granulation processes are carried out in batch and in continuous mode [33].

Systematic studies of granulation processes have been carried out for decades. Sand was the preferred material in early experimental studies [8, 9, 22]. These experimental studies were soon followed by works modelling the process [15, 16]. The growth of the particles is described by an early form of population balances and over the years the concept became well established [7, 12, 28]. With this tool, the particle ensemble is described on a

Table 1: *Unknown process parameters and their equivalent coded counterparts*

rate constant for	model variable	coded variable
coalescence	$\widehat{K}_0$	x_1
compaction	k_{porred}	x_2
breakage	$\widehat{k}_{\mathrm{att}}$	x_3
reaction	k_{reac}	x_4

per-particle basis, e. g. by the particle diameter. However, for wet granulation processes with particles consisting of more than one component these one-dimensional population balances are not sufficient enough to model the process [13]. In order to describe the particles in more detail, multidimensional descriptions are used [5, 10, 11, 24]. But besides from the details of the particle description, it is of major importance to capture, in any model, the transformations that are happening during the granulation. Wet granulation processes are considered to be governed by three subprocesses: Wetting and nucleation, coalescence and consolidation, and breakage and attrition [14].

The granulation of sugar pareils with water-polyethylene(PEG)-mixtures in a bench scale high shear mixer has been studied experimentally by [30]. This process was carried out under different conditions, i. e. a combination of different impeller speeds and binder compositions, with the outcome of the process being monitored for different process times. The water-PEG-ratio of the binder was 50/50, 70/30, and 90/10 wt%/wt% respectively and the mixer was operated at impeller speeds of 600, 900, and 1200 rpm. From a modelling point of view this process and these experimental investigations are interesting because of the varying process conditions. In addition to this, the setup requires a multidimensional particle description. This has been done in a previous study [6], representing the particles by a five-dimensional particle description accounting for two solids, two liquids and the pore volume of the granules. Such a detailed particle description is deemed necessary due to the various transformations being considered in the framework. Apart from coalescence and compaction, the particles can also undergo breakage. In addition to this, migration of liquid (penetration) and reaction within the granules is also allowed in the model. In order to compare the model with the experimental findings from [30], four process parameters (in this case kinetic constants) need to be established through fitting of the model to the experiments. As it can be computationally expensive to obtain model predictions from a full model, the process behaviour is approximated by linear response surfaces being functions of the four unknown process parameters. These parameters are rate constants for subprocesses, namely for coalescence, compaction, breakage and reaction and were already selected for an optimisation procedure in previous study [6] due to their eminence for the process. They appear as uncoded variables in the full granulation model and as coded variables in its approximation, i. e. the response surfaces. The naming of the variables in both models is given in **Table 1**. The mass of agglomerates was chosen as experimental observation and hence as criterion in the optimisation. Agglomerates are granules that exceed a certain size and were obtained from screening in the experiments. Further details of the full multidimensional population balance model and of the applied response surface methodology alongside a list with the parameters of the response surfaces can be found in [6]. In order to perform the estimation of the model uncertainty as

outlined above, the uncertainties associated with the experimental observations need to be known. As they are not available for the current data, they have to be estimated.

3.2 Estimation of experimental uncertainties

In order to demonstrate the application of the methodology, the unknown experimental uncertainties are estimated. Because the emphasis is on the method rather than on the details of the example, the chosen approach should be sufficient enough for demonstration purposes.

The experimental uncertainty σ_i^{exp} (of the ith observation) can originate from various sources. Despite the accuracy that an experimenter applies to an experiment, a small error is always introduced in every step of the experiment. For instance there will be an error weighing the raw materials and the product. Also during the process there will be deviation, e. g. in timing the process and therefore duration of mixing. As all these sources of uncertainty cannot be quantified, a relative uncertainty $\varsigma_{\text{rel}}^{\text{exp}}$ is used instead. The uncertainty σ_i^{exp} for the ith observation is computed by

$$\sigma_i^{\text{exp}} = \varsigma_{\text{rel}}^{\text{exp}}\, \eta_i^{\text{exp}} \qquad (i = 1, \ldots, N) \quad . \tag{18}$$

3.3 Further details of the optimisation procedure

As mentioned above, initial conditions and constraints have to be defined for the optimisation. The experimental design was set up in a previous study [6], so that the lower and upper limit for the coded variables become,

$$x_{0,k,\text{low}} = -1 \quad , \tag{19}$$

$$x_{0,k,\text{up}} = 1 \qquad (k = 1, \ldots, 4) \quad . \tag{20}$$

The centre of the experimental design is chosen as initial point for the model parameters,

$$\boldsymbol{x_0^{(0)}} = 0 \quad . \tag{21}$$

In addition to this, the uncertainty factors $\boldsymbol{c}$ have also initial values. We recall eq. (4),

$$x_k = x_{0,k} + c_k\, \xi_k \quad , \tag{4}$$

which becomes with the initial condition for $\boldsymbol{x_0}$

$$x_k = c_k\, \xi_k \quad . \tag{22}$$

Remembering that the random variable ξ_k is standard normally distributed, we can use the similarity with the experimental uncertainties. Hence, $x_k \in [-1 \;\; 1]$ is interpreted as one σ confidence interval of ξ_k, so that

$$c_k^{(0)} = 1 \quad . \tag{23}$$

$\boldsymbol{x_0^{(0)}}$ and $\boldsymbol{c^{(0)}}$ are called the unoptimised solution. The optimisation itself was carried out in Matlab using the function `fmincon`.

Table 2: *Mass of agglomerates (in grams) in experiments (binder composition water/PEG of 50/50 wt%/wt%)*

impeller speed [rpm]	time [s]			
	10	20	40	80
900	2.35	1.05	0.95	0.60
1200	1.60	0.80	0.50	0.40

Table 3: *Numbering scheme for experimental observations (binder composition water/PEG of 50/50 wt%/wt%)*

impeller speed	time [s]			
	10	20	40	80
900	1	2	3	4
1200	5	6	7	8

3.4 Results

In the previous study [6] 13 experimental observations were used in order to obtain the values for the four unknown process parameters ($x_1, \ldots, x_4$ or $\widehat{K}_0$, k_{porred}, $\widehat{k}_{\text{att}}$, and k_{reac} respectively), applying an optimisation procedure. These estimates were then used in further simulations in order to test and demonstrate the model's capability. However, the purpose of the current example is to show what the consequences of using the outlined methodology for uncertainty estimation are when applied to a wet-granulation model. As such, the influence of the choice of the experimental sets being used in the procedure is studied with respect to the obtained model parameters and their uncertainties, and subsequently for the model predictions and their uncertainties.

Only for the experimental data with a binder composition of water/PEG of 50/50 wt%/wt% measurements for different process times are available. **Table 2** lists the mass of agglomerates measured in the experiments. In a first step the data for the impeller speed of 900 rpm shall be used. In a second step, the observations from processes with an impeller speed of 1200 rpm are taken into consideration. In order to allow easy reference to the experimental cases/observations, a numbering scheme is applied (**Table 3**). As uncertainties for the experimental observations are not available, the relative uncertainty for every experimental observation is assumed to be $\varsigma_{\text{rel}}^{\text{exp}} = 0.3$.

We start off using set 1, i. e. one experimental observation, in order to specify the four unknown model parameters. Applying the outlined procedure results in a set of these parameters. This set can then be used for the computation of the model prediction of the mean value and its uncertainty using eqs. (10) and (11). In **Figure 2(a)** these data are plotted along with the experimental observation and the *a priori* estimate (unoptimised case). The latter is the initial guess for the model solution. The model prediction for the mass of agglomerates in this case is between 5 and 6 g, but at the same time the uncertainty is rather large. After optimisation the model prediction for the mass of agglomerates becomes smaller and identical with the experimental observation of 2.35 g. In addition to this, an uncertainty for the model prediction can be calculated, that is signifi-

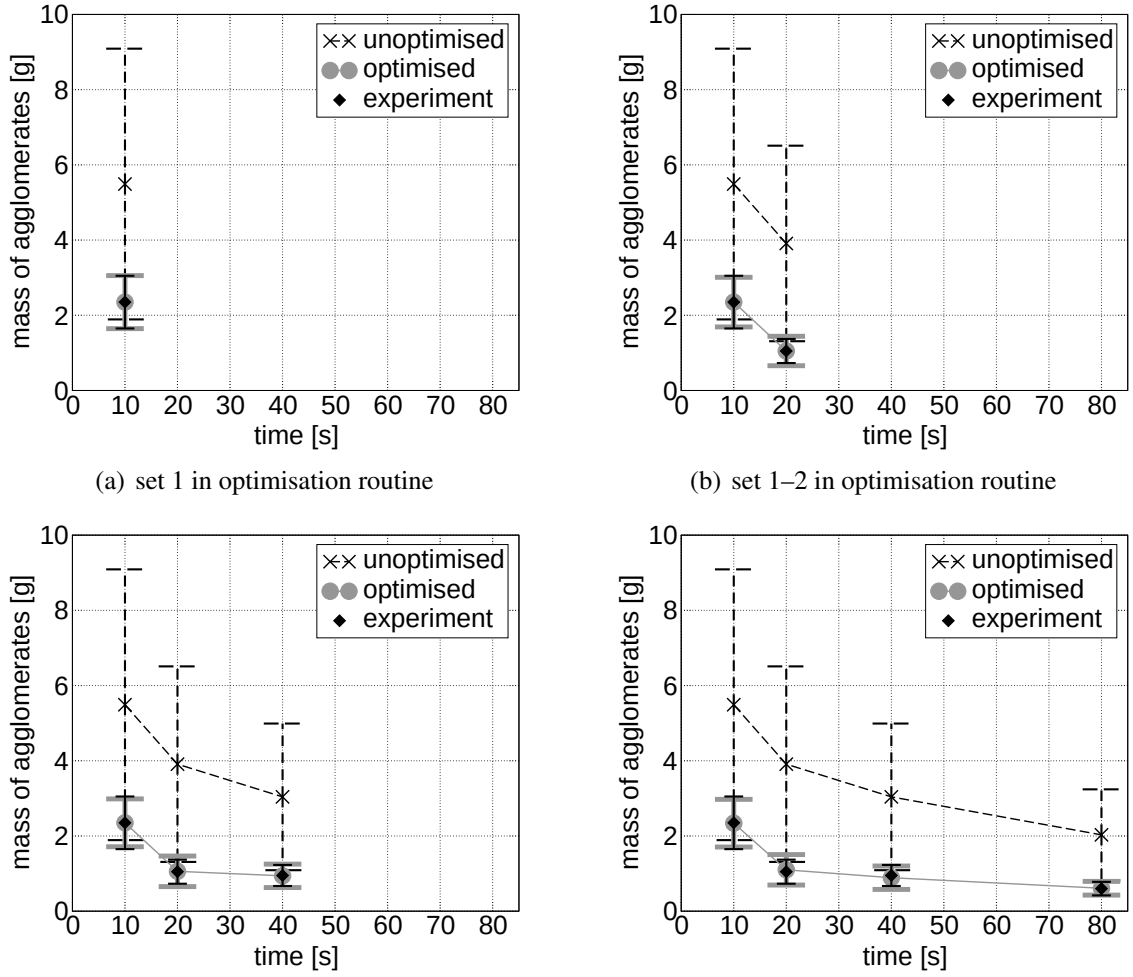

(a) set 1 in optimisation routine

(b) set 1–2 in optimisation routine

(c) set 1–3 in optimisation routine

(d) set 1–4 in optimisation routine

Figure 2: *Mass of agglomerates in the unoptimised and optimised model, and experiment (impeller speed of 900 rpm)*

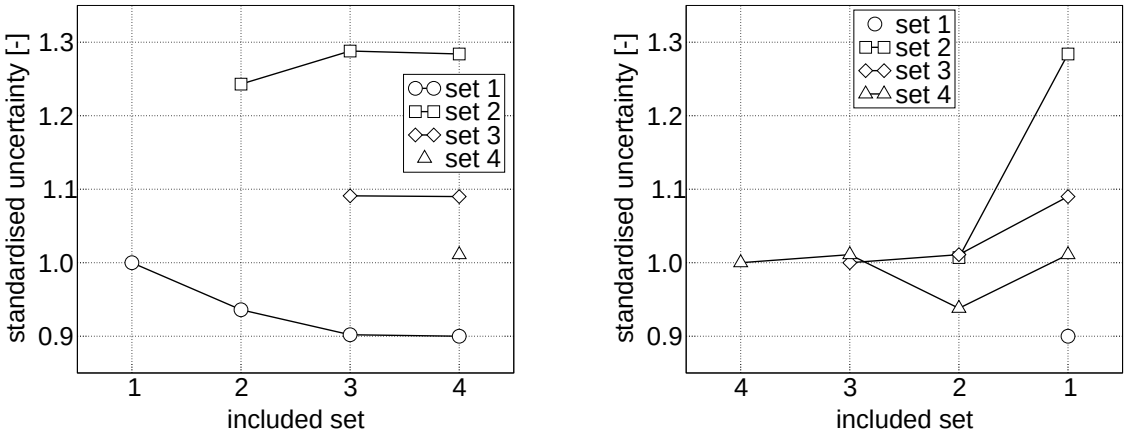

(a) Sets included in ascending order

(b) Sets included in descending order

Figure 3: *Standardised uncertainties for model predictions with optimised parameters—Set 1–4 of experimental observations successively included in optimisation procedure*

cantly smaller than the one for the unoptimised case. In fact, it takes the same value as the experimental uncertainty, as it should be expected since we are using one data point (cf. objective function eq. (14)). The entire procedure can now be repeated bringing in more experimental observations for the same process conditions, but different process times. The incorporation of set 2 to 4 in the optimisation leads to model predictions shown in **Figures 2(b)–2(d)**. In all cases the experimental observations are matched by the model very well. Also the uncertainties of the model predictions using the optimised parameters are significantly smaller compared to the *a priori* estimates. From this, it can be concluded that the model is appropriate in predicting the process outcome, provided the model parameters are chosen correctly.

One objective of the current study is the estimation of the uncertainty in the model parameters, and hence of the uncertainty in the model prediction. As these uncertainties are derived by using the experimental uncertainties, it is worthwhile to look how the uncertainties of the model predictions for a particular scenario are dependent upon the number of sets being used for the estimation of the uncertainties of the model parameters. Therefore a standardised uncertainty is defined as,

$$\text{standardised uncertainty} = \frac{\text{uncertainty of model prediction}}{\text{experimental uncertainty}} \quad . \tag{24}$$

For the cases just considered (set 1–4) this property is plotted in **Figure 3(a)**. This plot confirms the first impression of Figure 2 that the uncertainties do not change extensively between the different steps of the optimisation procedure. Turning to the standardised uncertainty of set 1, it can be observed that this is unity when just the experimental observation of set 1 is used for the estimation of the uncertainty of the model parameters and subsequently the model prediction. However, when set 2 is brought into consideration, a new set of uncertainty factors is derived leading to a smaller standardised uncertainty of the model prediction for set 1. In contrast to this, the same uncertainty factors yield for

set 2 a standardised uncertainty larger than unity. As a further set is brought into the procedure, a reduction in the uncertainty of the model prediction for set 1 can be observed, whereas it stays nearly constant at 90 % of the first value when all four sets are used for the estimation of the uncertainty factors. In contrast to this, the standardised uncertainties for the other three sets are always bigger than unity. For instance, the uncertainty in the model prediction for set 2 is nearly 30 % bigger than the experimental uncertainty. In order to understand why the standardised uncertainty can be bigger and smaller than unity, one has to recall how the uncertainty factors $\boldsymbol{c}$ are derived. In the optimisation we try to minimise the difference between the experimental uncertainty and the uncertainty of the model prediction for each set, and thereby extracting a common set of uncertainty factors $\boldsymbol{c}$ that are used for the computation of the model uncertainty σ_i for every scenario i,

$$\sigma_i(\boldsymbol{c}) = \sqrt{\sum_{k=1}^{K} \beta_{k,i}^2 \, c_k^2} \quad . \tag{25}$$

with $\beta_{k,i}$ being the kth parameter of the ith response surface. As such, the parameters $\beta_{k,i}$ can be considered as weights with respect to the different uncertainty factors. Due to the structure of eq. (25) and the fact that a common set of uncertainty factors $\boldsymbol{c}$ is used for the computation of each σ_i, the parameters $\beta_{k,i}$ of the ith scenario determine whether the standardised uncertainty becomes smaller or bigger than unity.

In the current example the sets 1 to 4 are included in ascending order in the procedure leading to the estimation of the model parameters and their uncertainties based on four observations when all sets are included. The same situation can be created by performing the procedure with a different start set, e. g. set 4, and subsequently include the other sets in descending order. The resulting trends for the standardised uncertainties are plotted in **Figure 3(b)**. The final points in Figure 3(a) and 3(b) are identical. However, without set 1 included in the procedure when using the sets in descending order (Figure 3(b)) the trends for the standardised uncertainties of the included sets are fairly close to unity, suggesting that the inclusion of set 1 in the procedure has a major effect on the estimation of the uncertainty factors. Nevertheless, using sets 1 to 4 in estimating the model parameters and their uncertainties demonstrates clearly that the proposed methodology works, which is built around exploiting the experimental uncertainties. As these are a centerpiece in estimating the uncertainties of the model prediction, it is on the one hand desirable to make sure that they are well deduced, and on the other hand one should aim to bring in more observations (incl. uncertainties) in order to broaden the basis for the estimation of the unknown parameters. Thereby it should be easier to identify outliers.

So far, only experimental observations from processes with the same process conditions but different times were included in the considerations. However, the influence of the impeller speed as a process condition is reflected in the granulation model, so that a common set of model parameters, i. e. rate constants, for different process conditions (in the current study the impeller speed) shall be established. Therefore the first set of the experiments with an impeller speed of 1200 rpm (set 5) is included in the optimisation procedure. The resulting set of optimised parameters leads to the model predictions in **Figures 4(b)** and **4(c)**. For an impeller speed of 900 rpm the model predictions in Figure 4(b) are still quite close to the experimental observations, although not as close as in the fit with just four sets (Figure 4(a)). However, the agreement between the experimental observation

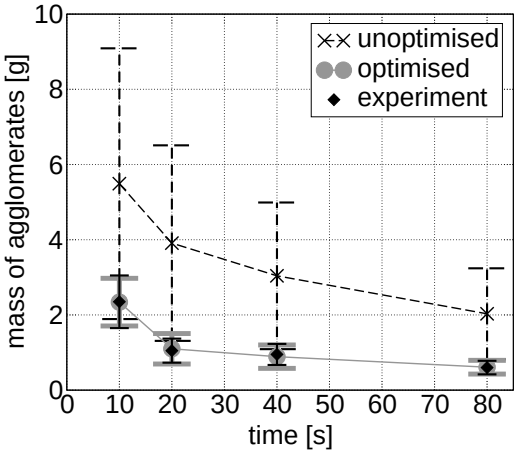

(a) 900 rpm, set 1–4 in optimisation routine

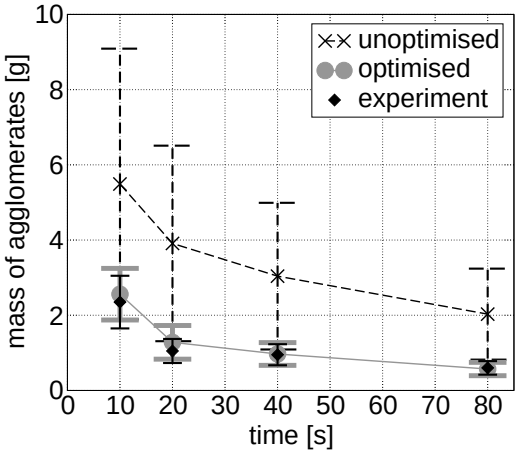

(b) 900 rpm, set 1–5 in optimisation routine

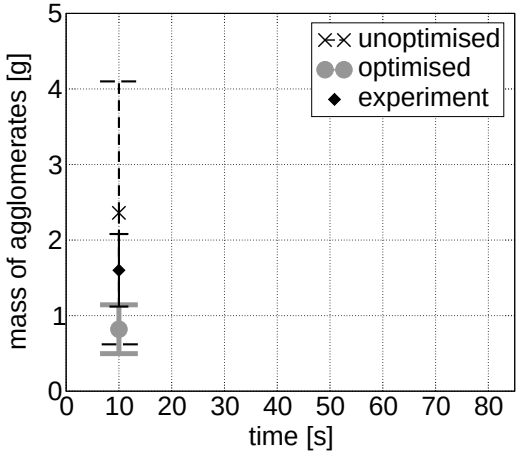

(c) 1200 rpm, set 1–5 in optimisation routine

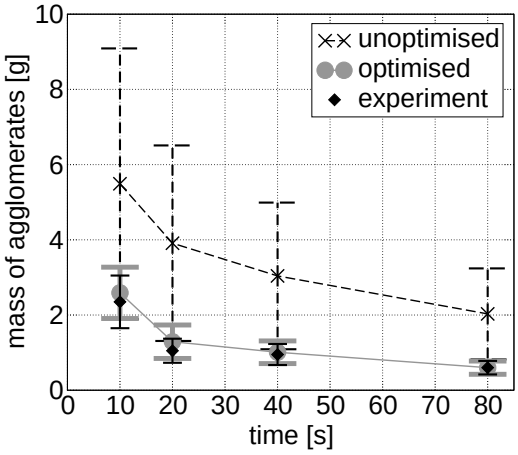

(d) 900 rpm, set 1–6 in optimisation routine

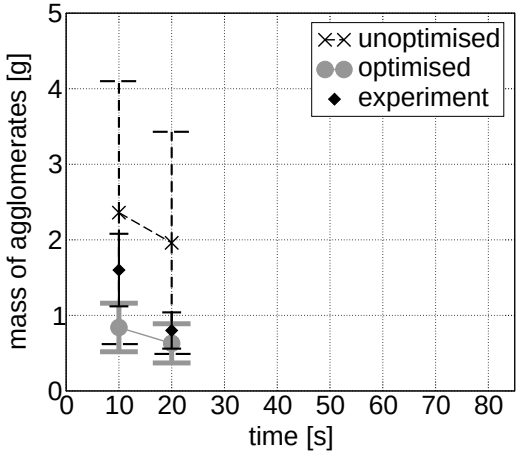

(e) 1200 rpm, set 1–6 in optimisation routine

Figure 4: *Mass of agglomerates in the unoptimised and optimised model, and experiment for setups with different impeller speed*

and the model prediction for set 5 (1200 rpm, 10 s) is not satisfying (**Figure 4(c)**). The agreement between model prediction and experimental observation would have been acceptable, if the experimental observation were to lie within the uncertainty bounds of the model prediction, which is clearly not the case for set 5. As it is the aim to find one set of model parameters that is applicable for all scenarios, the question comes up as to whether this can be found by including all sets in the methodology. The inclusion of a bigger number of sets, i. e. set 6, 7, and 8, results in parameter sets that lead to the model predictions shown in **Figure 4(d)–4(i)**. The model predictions for the cases with an impeller speed of 900 rpm are only altered marginally due to the inclusion of more experimental observations in the procedure (Figure 4(d), 4(f), and 4(h)). Reasonable agreement can be observed for the scenarios with an impeller speed of 1200 rpm, except for set 5, i. e. the experimental observations lie within the uncertainty bounds of the model predictions. But obviously there is a problem with set 5 and its model prediction after applying the optimisation procedure in which a new set of model parameters is found and the *a priori* model uncertainties are reduced to the present level. The mismatch between model prediction and experimental observation can originate from two sources. On the one hand there might be a problem with the experimental observation. This may have a very simple cause as for instance a misread number. Also one might want to check the experimental error of the observation. In the current case there is no information about this error, and so a value was assumed for it. Nevertheless, the value could be wrong, and one might have to think about its value again. However, if it is assumed that the experimental observation including the experimental error is correct as such, one should think about repeating the experiment, although this may not be appropriate or even possible. On the other hand, the problems might originate from the model chosen for the system of interest. This means it is inappropriate for a particular case. One has to remember that initially, limits for the choice of the unknown model parameters are introduced. Assuming that the "right" model parameter set lies within these ranges, one has to turn to the model itself. This means one has to revisit the assumptions and formulation of the model in order to capture a bigger set of problems, but keeping the required precision and robustness. With response surfaces being used as approximation for the full model, a source for errors is introduced in the system description. This means the response surface might not fully capture the features of the complex population balance model, and as result of this it contributes to the mismatch between model prediction and experiment observation. However, it is beyond the scope of the current study to revisit and refine the used models.

As we have identified a mismatch between the model prediction and the experimental observation for set 5, one may think about excluding this case from the procedure completely in order to investigate the behaviour of the remaining system. Of course, there is debate whether any data should ever be rejected, but in order to see what influence the exclusion of set 5 has on the entire methodology, it is done in this example. The model predictions for the model parameter set resulting from the procedure run with seven data sets are plotted in **Figure 5**. The difference between the predictions using parameter sets with and without set 5 are not huge. For the 900 rpm cases the match between experimental observations and model predictions and their uncertainties becomes better again (Figure 5(a) and 5(c)). Marginal changes can be observed for the 1200 rpm case (Figure 5(b) and 5(d)). The model predictions become slightly smaller than before. It is interesting to note that the experimental observation for set 6 (1200 rpm, 20 s) lies at the boundary

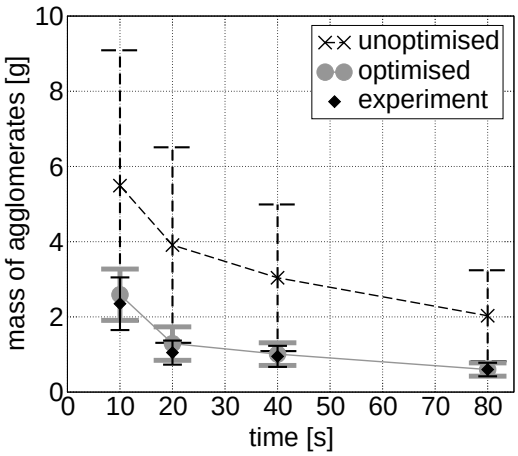

(d) 900 rpm, set 1–6 in optimisation routine

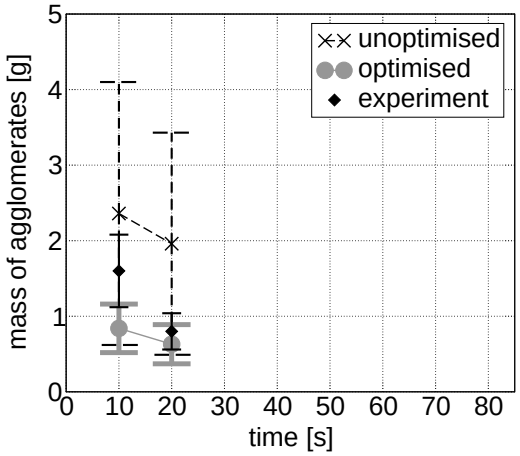

(e) 1200 rpm, set 1–6 in optimisation routine

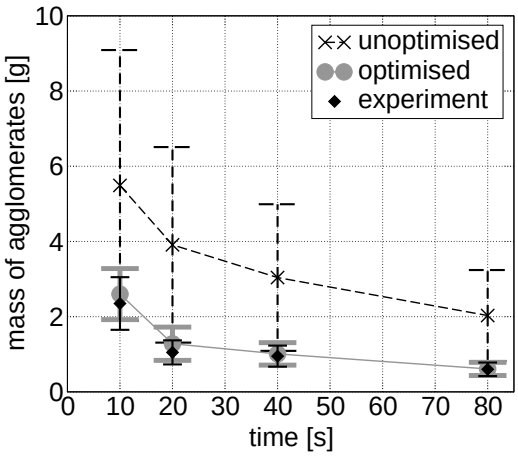

(f) 900 rpm, set 1–7 in optimisation routine

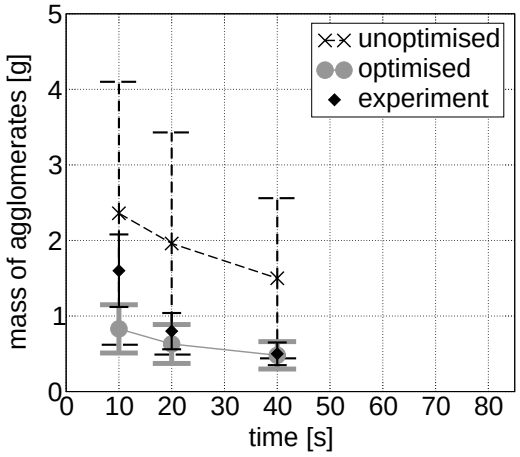

(g) 1200 rpm, set 1–7 in optimisation routine

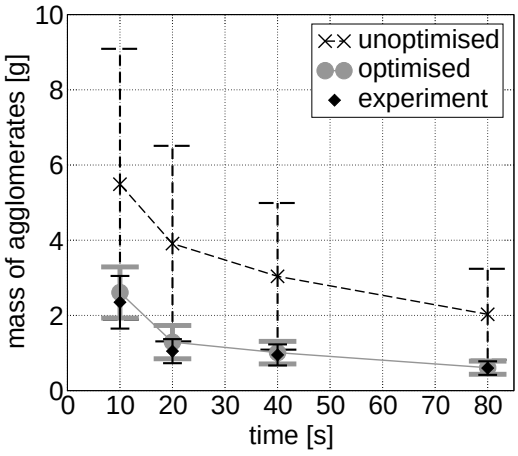

(h) 900 rpm, set 1–8 in optimisation routine

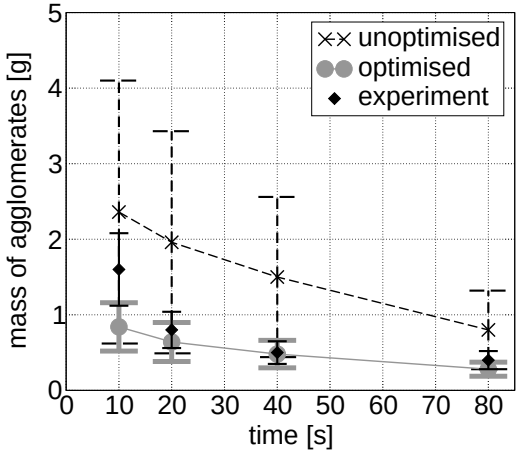

(i) 1200 rpm, set 1–8 in optimisation routine

Figure 4: *Mass of agglomerates in the unoptimised and optimised model, and experiment for setups with different impeller speed (cont.)*

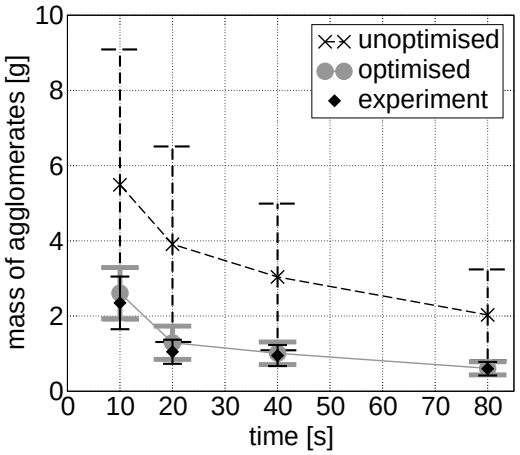

(a) 900 rpm, set 1–8 in optimisation routine

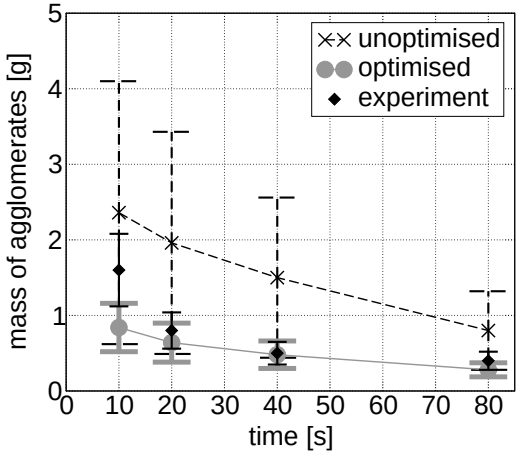

(b) 1200 rpm, set 1–8 in optimisation routine

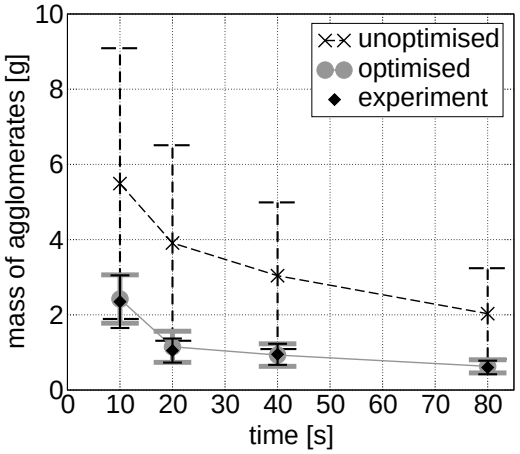

(c) 900 rpm, set 1–4 and 6–8 in optimisation routine

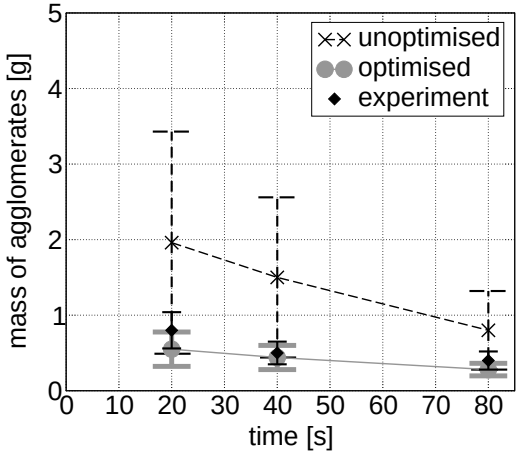

(d) 1200 rpm, set 1–4 and 6–8 in optimisation routine

Figure 5: *Mass of agglomerates in the unoptimised and optimised model, and experiment for rate constants estimated from all sets, but set 5 (1200 rpm, 10s)*

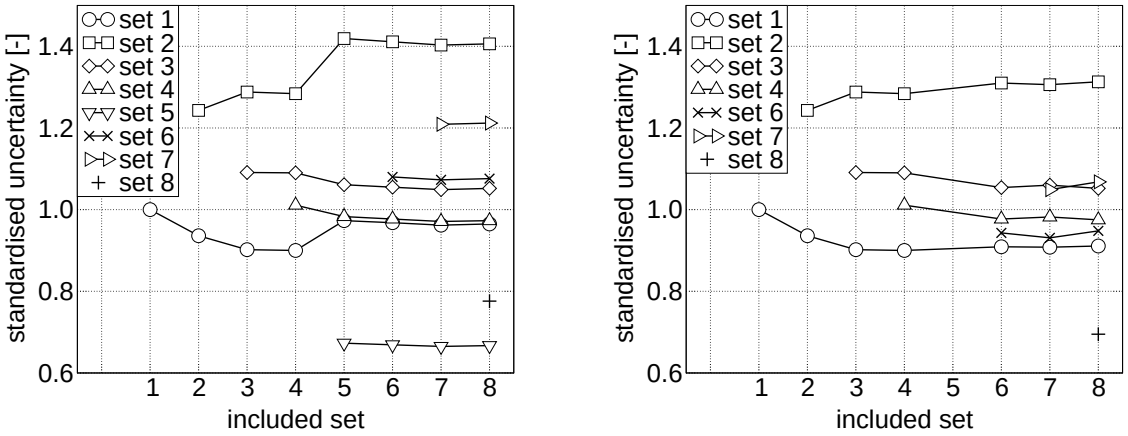

(a) all sets used

(b) all sets used except set 5

Figure 6: *Standardised uncertainties for model predictions with optimised parameters—Set 1–8 of experimental observations successively included in optimisation procedure*

of the uncertainty interval of the model prediction using the new set of model parameters (Figure 5(d)). This data point could potentially be a candidate for another review.

When using sets 1 to 4 for the estimation of the unknown model parameters and their uncertainties, some interesting trends for the evolution of the uncertainties of the model predictions can be observed as the number of sets in the procedure is increased. For the current case these uncertainties stabilise as sets 5 to 8 are included in the optimisation procedure (**Figure 6(a)**). However, when set 5 is brought into the procedure, the uncertainties of sets 1 and 2 increase. If set 5 is excluded from the optimisation procedure, such an increase in the standardised uncertainty does not occur (**Figure 6(b)**). This result highlights once more how the choice of the experimental basis has a direct impact on the values of the model parameters and hence on the model prediction and its uncertainty.

The model predictions for the mass of agglomerates depend on the model parameters $x_1, \ldots, x_4$ being obtained from the optimisation. The values of these parameters are dependent on the choice of the process conditions and experimental observations included in the optimisation procedure (**Table 4**). When being derived from set 1 to 4 (impeller speed of 900 rpm), the parameter values differ to some extent significantly between the different steps. However, when more experimental observations are brought into the consideration in steps 5 to 8, the solution stabilises around the final values for all eight sets. However, excluding set 5 in step 9 leads to a parameter set that is remarkably close to the one using just set 1 to 4 (Table 4, step 4).

A slightly different picture emerges for the uncertainties $\boldsymbol{c}$ of the process parameters (**Table 5**). Using the first four sets for the estimation of the unknown parameters $x_1, \ldots, x_4$ and their uncertainties means that there is no uncertainty for the rate constant for coalescence and reaction (x_1, x_4). The uncertainty of the model prediction is due to the uncertainty in the values of the model parameters for compaction and breakage (c_2, c_3). However, as soon as the fifth set (impeller speed of 1200 rpm) is brought into consideration, the uncertainty in the rate constant for breakage (x_3) ceases and the model un-

Table 4: *Sets used in the optimisation and the resulting values of the coded model parameters (▲ = active, △ = not used)*

	set											
step	1	2	3	4	5	6	7	8	x_1 [-]	x_2 [-]	x_3 [-]	x_4 [-]
1	▲	△	△	△	△	△	△	△	-0.5567	-0.6204	0.6468	0.3785
2	▲	▲	△	△	△	△	△	△	-0.8539	-0.4848	-0.5678	0.7254
3	▲	▲	▲	△	△	△	△	△	-0.7440	-1.0000	-0.8954	-1.0000
4	▲	▲	▲	▲	△	△	△	△	-0.6382	-1.0000	-0.5947	0.6425
5	▲	▲	▲	▲	▲	△	△	△	-0.8678	-0.2087	-0.4029	1.0000
6	▲	▲	▲	▲	▲	▲	△	△	-0.6338	-0.7656	-0.4966	1.0000
7	▲	▲	▲	▲	▲	▲	▲	△	-0.5387	-1.0000	-0.5388	1.0000
8	▲	▲	▲	▲	▲	▲	▲	▲	-0.5367	-1.0000	-0.5442	1.0000
9	▲	▲	▲	▲	△	▲	▲	▲	-0.6125	-1.0000	-0.5816	0.6891

Table 5: *Sets used in the optimisation and the resulting uncertainty factors of the coded model parameters (▲ = active, △ = not used)*

	set											
step	1	2	3	4	5	6	7	8	c_1 [-]	c_2 [-]	c_3 [-]	c_4 [-]
1	▲	△	△	△	△	△	△	△	0.0641	0.0815	0.9955	0.9999
2	▲	▲	△	△	△	△	△	△	0.0045	0.0018	0.9982	0
3	▲	▲	▲	△	△	△	△	△	0.0010	0.3908	0.4747	0
4	▲	▲	▲	▲	△	△	△	△	0	0.3886	0.4780	0
5	▲	▲	▲	▲	▲	△	△	△	0.0008	0.4848	0	0.0075
6	▲	▲	▲	▲	▲	▲	△	△	0	0.4820	0.0030	0
7	▲	▲	▲	▲	▲	▲	▲	△	0	0.4791	0	0.0014
8	▲	▲	▲	▲	▲	▲	▲	▲	0	0.4803	0	0.0026
9	▲	▲	▲	▲	△	▲	▲	▲	0	0.4231	0.3499	0.0071

Table 6: *Values for the model parameters and their uncertainties*

step	$\widehat{K}_0 \cdot 10^{10}$ [m^3]	k_{porred} [s m^{-1}]	$\widehat{k}_{\text{att}} \cdot 10^{-7}$ [s m^{-5}]	$k_{\text{reac}} \cdot 10^{9}$ [m s^{-1}]
1	1.22 ± 0.03	0.238 ± 0.008	7.3 ± 2.0	3.4 ± 1.0
2	1.073 ± 0.002	0.2515 ± 0.0002	4.9 ± 2.0	3.7 ± 0.0
3	1.1280 ± 0.0005	0.20 ± 0.04	4.2 ± 0.9	2.0 ± 0.0
4	1.18 ± 0.00	0.20 ± 0.04	4.8 ± 1.0	3.6 ± 0.0
5	1.0661 ± 0.0004	0.28 ± 0.05	5.2 ± 0.0	4.000 ± 0.008
6	1.18 ± 0.00	0.22 ± 0.05	5.007 ± 0.006	4.0 ± 0.0
7	1.23 ± 0.00	0.20 ± 0.05	4.9 ± 0.0	4.000 ± 0.001
8	1.23 ± 0.00	0.20 ± 0.05	4.9 ± 0.0	4.000 ± 0.003
9	1.19 ± 0.00	0.20 ± 0.04	4.8 ± 0.7	3.689 ± 0.007

certainty is basically governed by the uncertainty in the compaction rate constant (x_2). This behaviour does not change when the other three observations (sets 6-8) are used, too. However, when set 5 is excluded in step 9 (Table 5), the set of uncertainty factors is once again comparable with the one obtained for sets 1 to 4 only, although the match is not as good as for the set of model parameters.

One aim of this study is to establish the four unknown rate constants for a wet granulation problem. Therefore, the coded variables $\boldsymbol{x}$ and their uncertainties $\boldsymbol{c}$ have to be transformed into, up to now, unknown model parameters (with dimensions) for coalescence $\widehat{K}_0$, compaction k_{porred}, breakage $\widehat{k}_{\text{att}}$, and reaction k_{reac}. The optimised values for these parameters and their uncertainties are summarised in **Table 6**. The equations of how to transform the coded variables $\boldsymbol{x}$ and their uncertainties $\boldsymbol{c}$ into the "real" process parameters can be found in appendix A. A clear dependency of the values of the model parameters and their uncertainties on the choice of the experimental observations for their estimation can be observed.

4 Conclusions

A methodology that accounts for the propagation of experimental uncertainties into model predictions has been presented in this study and demonstrated for an example from high shear granulation. The process was modelled by a complex population balance framework which contains a myriad of model parameters. Four of these parameters needed to be established by comparison of model and experiments. As the experimental observations possess uncertainties, this should be reflected in the model predictions. In order to deal with this problem, a simple polynomial chaos expansion for the model parameters of interest was proposed, so that subsequently the expectation and variance of the model prediction could be derived and used in a straightforward optimisation step for the estimation of the uncertainties in the model parameters.

In the presented example, the process was approximated by linear response surfaces in order to allow fast computation of the model response in the optimisation procedure. The unknown model parameters are characteristics for the transformations that are incorpo-

rated in the model framework. As such, the rate constants for coalescence, compaction, breakage and reaction have been estimated by successively including eight sets of experimental observations in the procedure. At the same time the *a priori* uncertainties of the parameters and the model predictions have been reduced significantly by the methodology. The agreement between the model predictions using the estimated model parameters and the experimental observations was generally good. However, due to the employed methodology it was also possible to identify a mismatch between the model prediction and the experimental observation for one scenario. The reason for this can be twofold. One reason might be that the experimental observation is not correct, but if it is, the model lacks some important system description. In addition to this one has to be aware of the simplifications being might when using the response surfaces. Hence, not all features of the complex model might be fully captured. These problems have to be addressed in further work. Although this example is just demonstrating the methodology, further application for bigger systems is foreseeable.

Notation

c	uncertainty factor	[x]
E	expectation of the random variable X	$[X]$
K	number of model parameters	-
$\widehat{K}_0$	rate constant for coalescence	m^3
$\widehat{k}_{\mathrm{att}}$	rate constant for breakage	$\mathrm{s\,m}^{-5}$
k_{porred}	rate constant for compaction	$\mathrm{s\,m}^{-1}$
k_{reac}	rate constant for reaction	$\mathrm{m\,s}^{-1}$
M	number of random variables	-
N	number of experimental observations	-
Var	variance of the random variable X	$[X^2]$
X	random variable	$[X]$
x	model parameter	$[x]$
y	uncoded variable	$[y]$
δy	uncertainty of y	$[y]$

Greek letters

α	arbitrary constant	$[\alpha]$
β	parameter of response surface	$[\eta]$
η	model response	$[\eta]$
η^{exp}	experimental response	$[\eta^{\mathrm{exp}}]$
μ	model prediction	$[\eta]$
ξ	random variable	-
σ	uncertainty	$[\eta]$
ς_{rel}	relative uncertainty	-
Φ	objective function	$[\Phi]$

Superscripts

*	optimum
(0)	initial value
exp	experiment

Subscripts

0	base value
i	counting variable
k	counting variable
low	lower limit
up	upper limit

Acknowledgments

The authors would like to thank Procter and Gamble and the ESPRC (grant EP-E01772X) for financial support. They are also grateful for the fruitful discussions with Paul Mort and his colleagues at Procter and Gamble.

A Useful equations

A.1 Expectation and variance of response surfaces

In order to derive the expectation and variance of the response surfaces, following rules are used:

$$E\left(\sum_{i=1}^{M} \alpha_i \, X_i\right) = \sum_{i=1}^{M} \alpha_i \, E(X_i) \quad , \tag{26}$$

$$\mathrm{Var}\left(\sum_{i=1}^{M} \alpha_i \, X_i\right) = \sum_{i=1}^{M} \alpha_i^2 \, \mathrm{Var}\left(X_i\right) \quad , \tag{27}$$

with X_i being i.i.d. and α_i a set of constants ($i = 1, \ldots, M$). The model response η is a function of $\boldsymbol{x_0}$, $\boldsymbol{c}$, and $\boldsymbol{\xi}$,

$$\eta\left(\boldsymbol{x_0}, \boldsymbol{c}, \boldsymbol{\xi}\right) = \beta_0 + \sum_{k=1}^{K} \left(\beta_k \, x_{0,k} + \beta_k \, c_k \, \xi_k\right) \quad , \tag{28}$$

where $\boldsymbol{\xi}$ are the random variables. The expectation of η becomes then

$$E\left[\eta\left(\boldsymbol{x_0}, \boldsymbol{c}, \boldsymbol{\xi}\right)\right] = E\left(\beta_0 + \sum_{k=1}^{K} \beta_k \, x_{0,k}\right) + E\left(\sum_{k=1}^{K} \beta_k \, c_k \, \xi_k\right) \quad , \tag{29}$$

$$= \beta_0 + \sum_{k=1}^{K} \beta_k \, x_{0,k} + \sum_{k=1}^{K} \beta_k \, c_k \, E\left(\xi_k\right) \quad , \tag{30}$$

and with ξ_k being standard normally distributed the mean value μ becomes,

$$\mu(\boldsymbol{x_0}) = E\left[\eta\left(\boldsymbol{x_0}, \boldsymbol{c}, \boldsymbol{\xi}\right)\right] = \beta_0 + \sum_{k=1}^{K} \beta_k \, x_{0,k} \quad . \tag{31}$$

For the variance we obtain,

$$\mathrm{Var}\left(\eta\left(\boldsymbol{x_0}, \boldsymbol{c}, \boldsymbol{\xi}\right)\right) = \mathrm{Var}\left(\beta_0 + \sum_{k=1}^{K} \beta_k \, x_{0,k}\right) + \mathrm{Var}\left(\sum_{k=1}^{K} \beta_k \, c_k \, \xi_k\right) \quad , \tag{32}$$

$$= \sum_{k=1}^{K} \beta_k^2 \, c_k^2 \quad , \tag{33}$$

and subsequently the uncertainty σ equates to

$$\sigma(\boldsymbol{c}) = \sqrt{\mathrm{Var}\left(\eta\left(\boldsymbol{x_0}, \boldsymbol{c}, \boldsymbol{\xi}\right)\right)} = \sqrt{\sum_{k=1}^{K} \beta_k^2 \, c_k^2} \quad . \tag{34}$$

A.2 Transformation of coded into uncoded variables

The transformation of the coded variable x (dimensionless) into the corresponding uncoded variable y (with dimensions) is of linear nature. The experimental design is bound by x_{low} and x_{up} that correspond to the parameters from the physical world y_{low} and y_{up} respectively. Hence following relationship arises,

$$\frac{y - y_{\mathrm{low}}}{x - y_{\mathrm{low}}} = \frac{y_{\mathrm{up}} - y_{\mathrm{low}}}{x_{\mathrm{up}} - x_{\mathrm{low}}} \quad , \tag{35}$$

so that the uncoded variable y is expressed by,

$$y = \frac{y_{\mathrm{up}} - y_{\mathrm{low}}}{x_{\mathrm{up}} - x_{\mathrm{low}}} \left(x - x_{\mathrm{low}}\right) + y_{\mathrm{low}} \quad . \tag{36}$$

With the common case of $x_{\mathrm{low}} = -1$ and $x_{\mathrm{up}} = 1$ this relationship becomes,

$$y = \frac{y_{\mathrm{up}} - y_{\mathrm{low}}}{2} \left(x + 1\right) + y_{\mathrm{low}} \quad . \tag{37}$$

The uncertainty of y is denoted by δy. The uncertainty factor c expresses the uncertainty of the coded variable x. This means, it is equivalent to an Δx, so that

$$y(x_0 + \Delta x) = y(x_0) + \delta y \quad , \tag{38}$$

and hence

$$\delta y = y(x_0 + \Delta x) - y(x_0) \quad . \tag{39}$$

Inclusion of eq. (37) into eq. (39) leads to,

$$\delta y = \frac{y_{\text{up}} - y_{\text{low}}}{x_{\text{up}} - x_{\text{low}}}\, c \quad . \tag{40}$$

For $x_{\text{low}} = -1$ and $x_{\text{up}} = 1$ eq. (40) simplifies to,

$$\delta y = \frac{y_{\text{up}} - y_{\text{low}}}{2}\, c \quad . \tag{41}$$

References

[1] A. A. Adetayo, J. D. Litster, and M. Desai. The effect of process parameters on drum granulation of fertilizers with broad size distributions. *Chem. Eng. Sci.*, 48 (23):3951–3961, 1993. doi:10.1016/0009-2509(93)80374-Y.

[2] A. A. Adetayo, J. D. Litster, S. E. Pratsinis, and B. J. Ennis. Population balance modelling of drum granulation of material with wide size distribution. *Powder Technol.*, 82:37–49, 1995. doi:10.1016/0032-5910(94)02896-V.

[3] M. Banks and M. E. Aulton. Fluidized-bed granulation—A chronology. *Drug Dev. Ind. Pharm.*, 17(11):1437–1463, 1991.

[4] R. Boerefijn and M. J. Hounslow. Studies of fluid bed granulation in an industrial R&D context. *Chem. Eng. Sci.*, 60:3879–3890, 2005. doi:10.1016/j.ces.2005.02.021.

[5] A. Braumann, M. J. Goodson, M. Kraft, and P. R. Mort. Modelling and validation of granulation with heterogeneous binder dispersion and chemical reaction. *Chem. Eng. Sci.*, 62:4717–4728, 2007. doi:10.1016/j.ces.2007.05.028.

[6] A. Braumann, M. Kraft, and P. R. Mort. Applying response surface methodology to multidimensional granulation modelling, 2008. Technical Report 56, c4e-Preprint Series. Submitted to Powder Technology for publication.

[7] I. T. Cameron, F. Y. Wang, C. D. Immanuel, and F. Stepanek. Process systems modelling and applications in granulation: A review. *Chem. Eng. Sci.*, 60:3723–3750, 2005. doi:10.1016/j.ces.2005.02.004.

[8] C. E. Capes and P. V. Danckwerts. Granule formation by the agglomeration of damp powders—Part I: The mechanism of granule growth. *Trans. Instn Chem. Engrs*, 43: T116–T124, 1965.

[9] C. E. Capes and P. V. Danckwerts. Granule formation by the agglomeration of damp powders—Part II: The distribution of granules sizes. *Trans. Instn Chem. Engrs*, 43: T125–T130, 1965.

[10] A. Darelius, H. Brage, A. Rasmuson, I. N. Björn, and S. Folestad. A volume-based multi-dimensional population balance approach for modelling high shear granulation. *Chem. Eng. Sci.*, 61:2482–2493, 2006. doi:10.1016/j.ces.2005.11.016.

[11] M. Goodson, M. Kraft, S. Forrest, and J. Bridgwater. A multi-dimensional population balance model for agglomeration. In *PARTEC 2004—International Congress for Particle Technology*, 2004.

[12] M. J. Hounslow. The population balance as a tool for understanding particle rate processes. *KONA*, 16:179–193, 1998.

[13] S. M. Iveson. Limitations of one-dimensional population balance models of wet granulation processes. *Powder Technol.*, 124:219–229, 2002. doi:10.1016/S0032-5910(02)00026-8.

[14] S. M. Iveson, J. D. Litster, K. Hapgood, and B. J. Ennis. Nucleation, growth and breakage phenomena in agitated wet granulation processes: a review. *Powder Technol.*, 117:3–39, 2001. doi:10.1016/S0032-5910(01)00313-8.

[15] P. C. Kapur and D. W. Fuerstenau. Kinetics of green pelletization. *Transactions - Society of Mining Engineers of AIME*, 229:348–355, 1964.

[16] P. C. Kapur and D. W. Fuerstenau. A coalescence model for granulation. *I&EC Process Design and Development*, 8:56–62, 1969. doi:10.1021/i260029a010.

[17] P. L. W. Man, M. Kraft, and J. R. Norris. Coupling algorithms for calculating sensitivities of population balances. In T. E. Simos, G. Psihoyios, and C. Tsitouras, editors, *Numerical Analysis and Applied Mathematics*, volume 1048 of *AIP Conference Proceedings*, pages 927–930, 2008.

[18] D. C. Montgomery and G. C. Runger. *Applied statistics and probability for engineers*. John Wiley & Sons, Inc., New York, 3rd edition, 2003.

[19] P. Mort and G. Tardos. Scale-up of agglomeration processes using transformations. *KONA*, 17:64–75, 1999.

[20] P. R. Mort, S. W. Capeci, and J. W. Holder. Control of agglomerate attributes in a continuous binder-agglomeration process. *Powder Technol.*, 117:173–176, 2001. doi:10.1016/S0032-5910(01)00323-0.

[21] S. Mosbach, A. M. Aldawood, and M. Kraft. Real-time evaluation of a detailed chemistry HCCI engine model using a tabulation technique. *Combust. Sci. Technol.*, 180(7):1263–1277, 2008. doi:10.1080/00102200802049414.

[22] D. M. Newitt and J. M. Conway-Jones. A contribution to the theory and practice of granulation. *Trans. Instn Chem. Engrs*, 36:422–441, 1958.

[23] B. D. Phenix, J. L. Dinaro, M. A. Tatang, J. W. Tester, J. B. Howard, and G. J. McRae. Incorporation of parametric uncertainty into complex kinetic mechanisms: Application to hydrogen oxidation in supercritical water. *Combust. Flame*, 112: 132–146, 1998. doi:10.1016/S0010-2180(97)81762-2.

[24] J. M.-H. Poon, C. D. Immanuel, F. J. Doyle III, and J. D. Litster. A three-dimensional population balance model of granulation with a mechanistic representation of the nucleation and aggregation phenoma. *Chem. Eng. Sci.*, 63:1315–1329, 2008. doi:10.1016/j.ces.2007.07.048.

[25] D. Ramkrishna and A. W. Mahoney. Population balance modeling. Promise for the future. *Chem. Eng. Sci.*, 57:595–606, 2002. doi:10.1016/S0009-2509(01)00386-4.

[26] M. T. Reagan, H. N. Najm, R. G. Ghanem, and O. M. Knio. Uncertainty quantification in reacting-flow simulations through non-intrusive spectral projection. *Combust. Flame*, 132:545–555, 2003. doi:10.1016/S0010-2180(02)00503-5.

[27] C. F. W. Sanders, A. W. Willemse, A. D. Salman, and M. J. Hounslow. Development of a predictive high-shear granulation model. *Powder Technol.*, 138:18–24, 2003. doi:10.1016/j.powtec.2003.08.046.

[28] K. V. S. Sastry. Similarity size distribution of agglomerates during their growth by coalescence in granulation or green pelletization. *Int. J. Miner. Process.*, 2:187–203, 1975.

[29] D. A. Sheen, X. You, H. Wang, and T. Løvås. Spectral uncertainty quantification, propagation and optimization of a detailed kinetic model for ethylene combustion. *Proc. Combust. Inst.*, 32(1):535–542, 2009. doi:10.1016/j.proci.2008.05.042.

[30] T. Simmons, R. Turton, and P. Mort. An investigation into the effects of time and shear rate on the spreading of liquids in coating and granulation processes. In *Fifth World Congress on Particle Technology*, 2006.

[31] G. I. Tardos, M. I. Khan, and P. R. Mort. Critical parameters and limiting conditions in binder granulation of fine powders. *Powder Technol.*, 94:245–258, 1997. doi:10.1016/S0032-5910(97)03321-4.

[32] A. Varma, M. Morbidelli, and H. Wu. *Parametric sensitivity in chemical systems*. Cambridge University Press, Cambridge, 1st edition, 1999.

[33] C. Vervaet and J. P. Remon. Continuous granulation in the pharmaceutical industry. *Chem. Eng. Sci.*, 60:3949–3957, 2005. doi:10.1016/j.ces.2005.02.028.

[34] A. Vikhansky and M. Kraft. A Monte Carlo methods for identification and sensitivity analysis of coagulation processes. *J. Comput. Phys.*, 200:50–59, 2004. doi:10.1016/j.jcp.2004.03.006.

[35] A. Vikhansky and M. Kraft. Two methods for sensitivity analysis of coagulation processes in population balances by a Monte Carlo method. *Chem. Eng. Sci.*, 61: 4966–4972, 2006. doi:10.1016/j.ces.2006.03.009.

[36] A. Vikhansky, M. Kraft, M. Simon, S. Schmidt, and H.-J. Bart. Droplets population balance in a rotating disc contactor: An inverse problem approach. *AIChE J.*, 52(4): 1441–1450, 2006. doi:10.1002/aic.10735.

[37] P. A. L. Wauters, R. van de Water, J. D. Litster, G. M. H. Meesters, and B. Scarlett. Growth and compaction behaviour of copper concentrate granules in a rotating drum. *Powder Technol.*, 124:230–237, 2002. doi:10.1016/S0032-5910(02)00029-3.

[38] D. Xiu and G. E. Karniadakis. The Wiener–Askey polynomial chaos for stochastic differential equations. *SIAM J. Sci. Comput.*, 24(2):619–644, 2002. doi:10.1137/S1064827501387826.